

Original Article

System analysis of metabolism and the transcriptome in *Arabidopsis thaliana* roots reveals differential co-regulation upon iron, sulfur and potassium deficiency

Ilaria Forieri¹, Carsten Sticht², Michael Reichelt³, Norbert Gretz², Malcolm J. Hawkesford⁴, Mario Malagoli⁵, Markus Wirtz¹ & Ruediger Hell¹

¹Centre for Organismal Studies (COS), University of Heidelberg, 69120 Heidelberg, Germany, ²Center for Medical Research, University of Mannheim, 68167 Mannheim, Germany, ³Max Planck Institute for Chemical Ecology, 07745 Jena, Germany, ⁴Rothamsted Research, Harpenden AL5 2JQ, UK and ⁵Department of Agronomy, Food, Natural Resources, Animals and Environment, University of Padova, Padua, Italy

ABSTRACT

Deprivation of mineral nutrients causes significant retardation of plant growth. This retardation is associated with nutrient-specific and general stress-induced transcriptional responses. In this study, we adjusted the external supply of iron, potassium and sulfur to cause the same retardation of shoot growth. Nevertheless, limitation by individual nutrients resulted in specific morphological adaptations and distinct shifts within the root metabolite fingerprint. The metabolic shifts affected key metabolites of primary metabolism and the stress-related phytohormones, jasmonic, salicylic and abscisic acid. These phytohormone signatures contributed to specific nutrient deficiency-induced transcriptional regulation. Limitation by the micronutrient iron caused the strongest regulation and affected 18% of the root transcriptome. Only 130 genes were regulated by all nutrients. Specific co-regulation between the iron and sulfur metabolic routes upon iron or sulfur deficiency was observed. Interestingly, iron deficiency caused regulation of a different set of genes of the sulfur assimilation pathway compared with sulfur deficiency itself, which demonstrates the presence of specific signal-transduction systems for the cross-regulation of the pathways. Combined iron and sulfur starvation experiments demonstrated that a requirement for a specific nutrient can overrule this cross-regulation. The comparative metabolomics and transcriptomics approach used dissected general stress from nutrient-specific regulation in roots of *Arabidopsis*.

INTRODUCTION

Acquisition of mineral nutrients by plants is of crucial importance for growth and ultimately yield. Plant responses towards deficiency of single minerals have been investigated intensively with respect to all essential nutrients. Analyses ranging from the phenotypic to the molecular level have revealed nutrient-specific response patterns but also a high degree of

commonality between the different long-term nutrient deficiencies. The existence of such a general nutrient-deficiency response was suggested to be triggered by the often observed increase of reactive oxygen species in nutrient-deprived roots (Schachtman & Shin 2007). Additionally, the elevation of the phytohormone ethylene in roots upon limitation of many nutrients, including iron (Fe), phosphorus (P), potassium (K), nitrogen (N) and sulfur (S), indicates the existence of a common response to nutrient deprivation (Garcia *et al.* 2015). Furthermore, the comparison of proteomic studies from P, N, Fe and K limitation points to a response for a common group of proteins (Liang *et al.* 2013). This concept of a general nutrient-deficiency response is supported by the induction of gene expression for P, K and Fe uptake systems under the deficiency of any one of these nutrients (Wang *et al.* 2002). A bioinformatics comparison of publicly available transcriptome analyses of N, P, K and S depleted plants revealed many similarities, indicating the recruitment of existing regulatory programmes for nutrient-starvation responses. A prominent part of this common transcriptional response is termed general nutrient-depletion-induced senescence (Watanabe *et al.* 2010). In addition to specific and common responses, interactions between deficiencies of single nutrient have been reported. Such an interaction is revealed by comprehensive transcriptome and metabolome analyses of plant responses towards N and S (Hirai *et al.* 2004). A connection between metabolism of molybdenum and iron is assumed based on the interaction of uptake mechanisms for molybdate and Fe, and the many enzymes that require molybdenum cofactor and iron-sulfur clusters (Bittner 2014).

Recent investigations suggest that the uptake systems for S and Fe are more coordinated than other nutrient uptake machineries (Astolfi *et al.* 2010, Astolfi *et al.* 2012, Zuchi *et al.* 2015), possibly because the most important sinks for Fe in cells are the diverse Fe-S clusters in proteins (Balk & Schaedler 2014, Forieri *et al.* 2013, Viganì & Briat 2015). Biosynthesis of Fe-S clusters takes place in plastids, in mitochondria and in the cytosol. The intermediate donor of Fe is unknown as yet, but cysteine has been identified as the sole S-donor for Fe-S

Correspondence: R. Hell. Phone: +49 6221 54 6284, Fax: +49 6221 54 5859; e-mail: ruediger.hell@cos.uni-heidelberg.de

cluster synthesis in organelles (reviewed by Balk & Schaedler 2014). Due to the high requirement for Fe-S clusters in the electron transport chains of both mitochondria and chloroplasts, feedback signals may originate from the organelles to regulate uptake and assimilation in response to nutrient availability (Balk & Schaedler 2014). Such signals have been hypothesized to play a fundamental role in both Fe and S assimilation (Chan *et al.* 2013, Vigani & Briat 2015).

In this study, limitations of Fe, S and in parallel K were applied to resolve specific cross-talk between nutrient uptake systems from the general responses of plant roots towards growth limitation. K was chosen as a control nutrient because deficiency has a strong impact on plant growth, but in contrast to other essential macronutrients, it is not assimilated or incorporated into organic compounds (Amtmann & Armengaud 2009). The study was designed such that in spite of different internal demands, depletion of each single nutrient by external supply caused the same loss of shoot biomass. This was seen as an essential prerequisite with respect to comparability of the effects of the nutrient stresses. Furthermore, the approach enabled the determination of insights on the specificity of the interaction between Fe and S that had not been considered in comparable nutrient-deficiency studies in other plant species (Astolfi *et al.* 2010, Astolfi *et al.* 2012, Zuchi *et al.* 2015). The responses to the three nutrient deficiencies were compared in a systematic approach based on transcriptome and metabolome analyses. The comprehensive metabolome analyses revealed nutrient-deficiency-specific responses of sulfur metabolism-

related metabolites. Furthermore, it uncovered characteristic profiles of stress-related phytohormones in roots that were almost entirely conserved in shoots and were likely to contribute to the specific regulation of the transcriptome during each nutrient-deficiency stress. Only a marginal number of genes were regulated in common upon growth limitation caused by the three different nutrient deficiencies. In contrast to the K-deficiency response, the responses to S and Fe deficiency shared a significant degree of cross-talk. The jointly regulated genes of Fe and S starvation included co-regulated and oppositely regulated genes.

RESULTS

Phenotypic analysis of nutrient-deficient plants

The three nutrient deficiencies tested induced specific phenotypical adaptations of leaves (Fig. 1a) when compared with the control condition (Ctrl), but all resulted in the same decrease of shoot fresh weight (FW) (approximately 6-fold; Fig. 1b). However, each nutrient deficiency had a specific impact on root FW (Fig. 1c): S-deprivation decreased root biomass 2-fold, and both iron and potassium deficiency, 6-fold. Consequently, the calculated root to shoot ratio (Fig. 1d) increased specifically upon S deficiency. Since the uptake of the analysed nutrients occurs solely by the root, further analysis was focused on this organ.

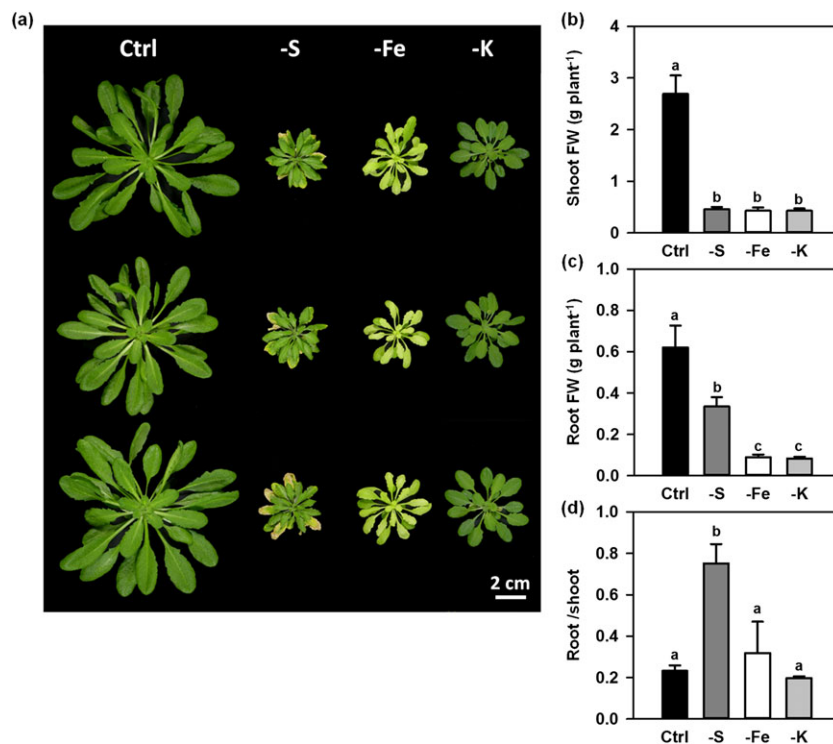


Figure 1. The applied deprivation of S, Fe and K results in specific adaptations but the same retardation of shoot growth. (a) Phenotype of 7-week-old *Arabidopsis thaliana* plants hydroponically grown under different nutritional regimes (Ctrl, full nutrient supply; -S, sulfur deficiency; -Fe, iron deficiency; -K, potassium deficiency). (b–d) Impact of nutrient deficiencies on fresh weight (FW) of the shoot (b), the roots (c) and root/shoot ratio (d). Data are means \pm SE of 10 individual replicates. Lettering indicates statistical differences by ANOVA ($P < 0.05$) as determined by Student–Newman–Keuls test.

Impact of different nutrient deficiencies on nutrient and anion concentrations

S deficiency caused a strong decrease of total S and sulfate in roots (Fig. 2a,b) and was accompanied by 1.5-fold increase of total P. This significant increase can be at least partly explained by the 3-fold accumulation of free phosphate (Fig. 2c). The applied Fe-deficiency condition resulted in a more than 6-fold lower Fe content in roots and strong accumulation of Cu and Zn. Total S increased in roots of Fe-deficient plants without affecting sulfate concentration. Both S and Fe deficiency caused a significant increase of total molybdenum (Mo). The only known biological function of Mo in plants is the presence in the Mo/Co-factor. Fe and S play an important role in the synthesis of this factor, since efficient Mo/Co factor synthesis requires the Fe-S cluster containing enzyme CNX2 and the mitochondrial ABC transporter ATM3 (Bittner 2014).

Importantly, retardation of plant growth by K-deficiency did not affect total Fe or S content. All applied nutrient deficiencies resulted in lower steady state nitrate levels (Fig. 2d).

Metabolic response of nutrient-deficient roots

The specific impact of different nutrient deficiencies on the primary metabolism was further investigated by determination of primary and secondary sulfur-related metabolites (Fig. 3a) and the proteinogenic amino acids. Despite a specific decrease of Ala and Asp, the K-deficiency response caused significant increase in content of total amino-acids (Supporting Information Fig. S1) and of reduced sulfur containing metabolites (Fig. 3c–g,j,k). The latter explained the unchanged total S-content of K-deprived roots, because sulfate, the most abundant S-containing metabolite of plant cells, was significantly decreased (Fig. 2a,b), and demonstrated a shift of sulfur from the oxidized to the reduced state.

All reduced S-containing metabolites decreased significantly upon S deficiency (Fig. 3c–h,j,k), which is a classical response of plants to S-deprivation in shoots and roots. The strongest decrease (23-fold) was observed for the total glucosinolate pool (Fig. 3e) and was mainly driven by a striking decrease of aliphatic glucosinolates to undetectable levels (Supporting Information Table S1). The C/N-containing skeleton for Cys synthesis, OAS, significantly accumulated under S deficiency (140-fold) as a result of decreased sulfide availability. Interestingly, Fe deficiency also caused an increase in OAS concentration compared with the control (14-fold), whereas K deficiency did not alter the OAS level (Fig. 3b). The availability of S and the significantly higher level of OAS in the -Fe condition resulted in higher steady state levels of Cys (Fig. 3d), Met (Fig. 3g) and S-adenosylmethionine (SAM; Fig. 3j). The increased SAM would facilitate a flux into the metal chelator nicotianamine (NA), which indeed accumulated strongly and specifically upon Fe-deficiency (10-fold; Fig. 3i). In contrast to the vast majority of methyl-transfer reactions that form S-adenosylhomocysteine (SAH) as a byproduct of SAM consumption, the use of SAM for synthesis of NA results in the formation of methylthioadenosine (MTA; reviewed in Sauter *et al.* 2013). The enhanced MTA level (Fig. 3f) indicated

(a)

Nutrient	Treatment		
	-S	-Fe	-K
S	-4.0*	1.8*	1.3
K	1.3	1.1	-3.4*
Ca	1.2	1.0	1.1
Mg	1.3	1.3	2.0*
P	1.5*	1.1	1.3
Fe	1.0	-6.4*	1.2
Cu	2.9	33.4*	1.3
Mn	1.0	1.2	1.1
Mo	5.0*	1.8*	1.2
Zn	1.2	2.9*	1.8

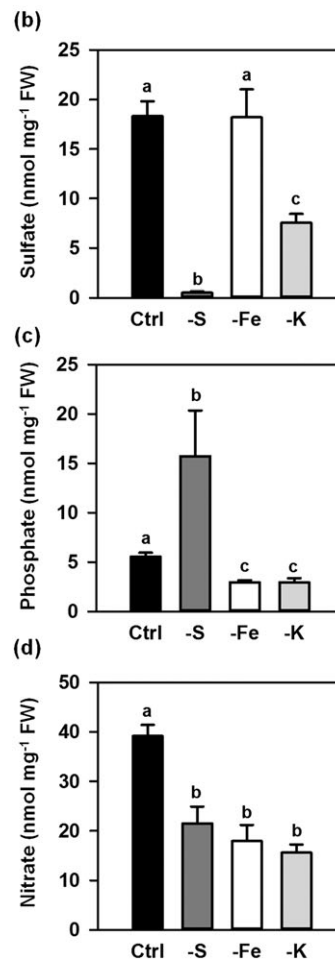


Figure 2. Deprivation of S, Fe or K impacts the overall nutritional status of roots. (a) Nutrient concentrations in roots of 7-week-old Arabidopsis wild-type plants that were grown on full nutrient supply (Ctrl) and depletion of sulfur (-S), iron (-Fe) and potassium (-K) as specified in material and methods. Data represent means ($n = 5$) and are converted into x-fold change compared with Ctrl. Steady state levels of nutrients ($\mu\text{g g}^{-1}$ DW) in Ctrl were as follows: sulfur (S), 8836; potassium (K), 36929; calcium (Ca), 7172; magnesium (Mg), 2057; phosphorous (P), 8146; iron (Fe), 288; copper (Cu), 19; manganese (Mn), 172; molybdenum (Mo), 54; zinc (Zn), 169. (b–d) Steady state levels of sulfate (b), phosphate (c) and nitrate (d) in the same roots as defined in A. Data are means \pm SE ($n = 4$). Asterisks (a) and lettering (b–d) indicates statistical differences by ANOVA ($P < 0.05$) as determined by Student–Newman–Keuls test.

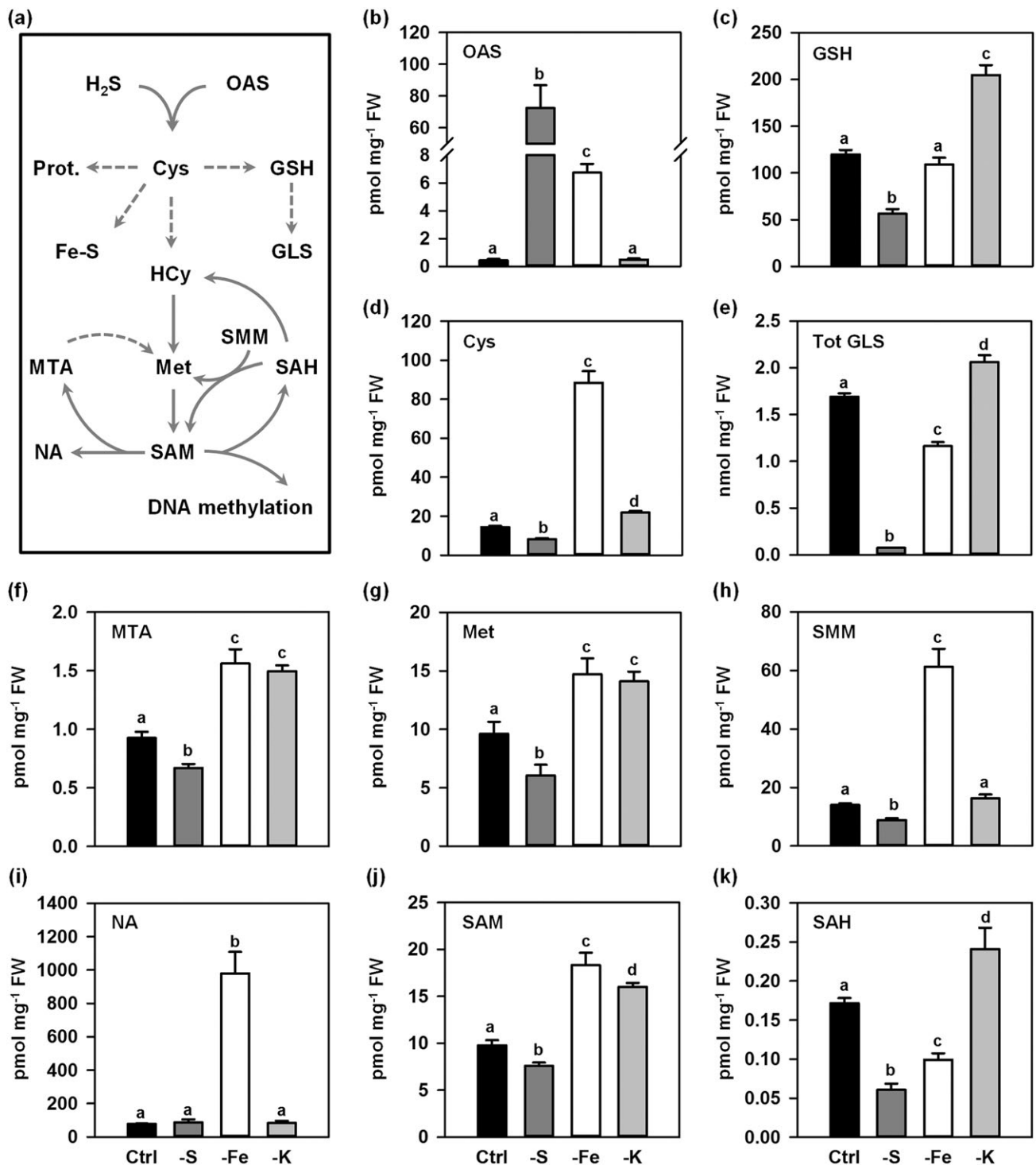


Figure 3. Deprivation of S, Fe or K results in specific adaptations within core S metabolism. (a) Schematic representation of Cys biosynthesis and down-stream metabolic sinks. Arrows indicate multi-step (dashed) or single reactions (continuous). (b–k) Steady state levels of O-acetylcysteine (b), glutathione (c), Cys (d), total glucosinolates (e), methylthioadenosine (f), Met (g), S methylmethionine (h), nicotianamine (i), S adenosylmethionine (j) and S-adenosylhomocysteine (k) in roots of seven week-old *Arabidopsis* wild-type plants that were grown on full nutrient supply (Ctrl, black bar) and depletion of sulfur (-S, dark grey), iron (-Fe, white) and potassium (-K, light grey) as specified in material and methods. Data are means \pm SE of more than four individual replicates. Lettering indicates statistical differences by ANOVA ($P < 0.05$) as determined by Student–Newman–Keuls test.

recycling of the S-moiety of SAM by the Yang-cycle in roots of Fe-depleted plants due to excessive formation of NA. In contrast to MTA, SAH decreased in Fe-deficient conditions

(Fig. 3k) and caused a significant increase of the methylation index (SAM/SAH ratio). This index is known to correlate with the methylation status of essential molecules such as RNA,

DNA and histones (Sauter *et al.* 2013). Alteration of DNA and histone methylation might contribute to the large perturbation of transcription under Fe-deficiency (see the succeeding texts). Efficient recycling of SAH to Met might be favoured in Fe-deficient roots by the enhanced level of S-methylmethionine (SMM; Fig. 3h), an abundant phloem mobile transport-form of reduced sulfur and carbon1-units that is used in the SMM cycle for conversion of SAH into SAM (Fig. 3a) (reviewed in Sauter *et al.* 2013).

Impact of nutrient deficiencies on the root phytohormone system

Control of nutrient uptake systems and other nutrient-deficiency-induced responses by the phytohormone system is strongly suggested by pharmacological treatment of roots with specific phytohormones (Barberon *et al.* 2016, Maruyama-Nakashita *et al.* 2004). Several transcriptome analyses found up-regulation of genes related to hormone synthesis during Fe, S or K deficiency and investigations of mutants deficient in hormone synthesis or perception (e.g. *brx* and *acs* mutant) revealed altered nutrient-deficiency responses (reviewed in Brumbarova *et al.* 2015, Koprivova & Kopriva 2016 and Wang & Wu 2013). However, information on the global changes of the endogenous root phytohormone system in response to nutrient supply is almost absent. The response of the stress-related hormones abscisic acid (ABA), salicylic acid (SA) and jasmonic acid (JA) to -F, -S or -K in the root as the primary site of nutrient uptake was highly specific (Fig. 4 and Supporting Information Fig. S2). ABA was only detectable in roots of

hydroponically grown plants that were subjected to K deprivation, which strongly indicates a significant induction of ABA production upon K deficiency (Fig. 4a). SA level increased significantly in response to -S and -K. In contrast Fe deficiency caused a significant decrease of SA in roots (Fig. 4b). Furthermore, JA and its derivatives decreased almost 10-fold in response to Fe deficiency when compared with S or K deficiency, which both had only minor impacts on JA levels in roots (Fig. 4c,d and Supporting Information Fig. S2). These results reveal specific alteration of the phytohormone signature in response to the applied nutrient deprivations in roots. Such a nutrient specific response of the phytohormone system was also detected in shoots, although all nutrient deficiencies caused the same limitation of growth in this organ (Fig. 4e–h). The Fe-deficiency-induced and K-deficiency-induced alterations of the phytohormone system were conserved between roots and shoots. In contrast, sulfur deficiency resulted in a significantly different phytohormone signature in roots when compared with shoots (Fig. 4). No obvious correlation was observed between the root-to-shoot ratio and the nutrient-induced alteration of the phytohormone signature.

Transcriptional responses of nutrient-deficient roots

Global transcriptome analyses were performed to investigate whether the growth limitation by the different nutrient deficiencies triggered specific or similar transcriptional responses (Fig. 5; Supporting Information Table S2, which lists the mean values calculated from the normalized expression values of the

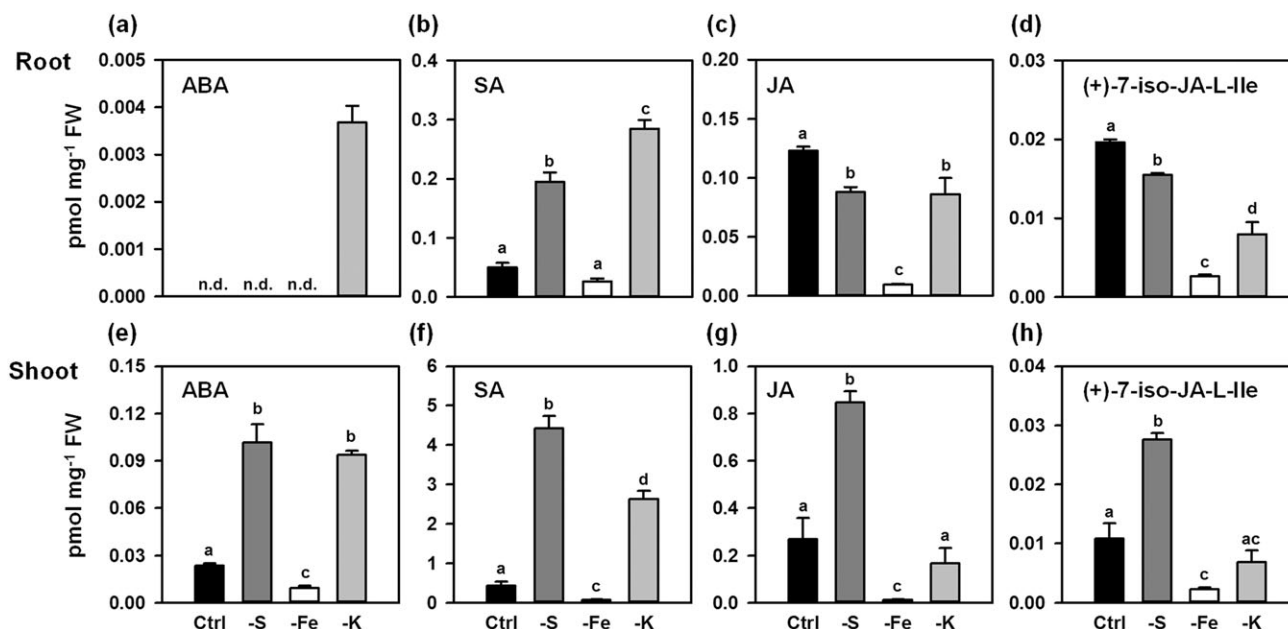


Figure 4. Different nutrient deprivations induce highly specific phytohormone signatures in roots. (a–h) Steady state levels of abscisic acid (a, e), salicylic acid (b, f), jasmonic acid (c, g) and (+)-7-iso-Ja-Ile (d, h) in roots (a–d) and shoots (e–h) of 7-week-old *Arabidopsis* plants that were grown on full nutrient supply (Ctrl, black bar) or medium depleted of sulfur (-S, dark grey), iron (-Fe, white) or potassium (-K, light grey) as specified in material and methods. Data are means \pm SE of more five individual replicates. Lettering indicates statistical differences by ANOVA ($P < 0.05$) as determined by Student–Newman–Keuls test.

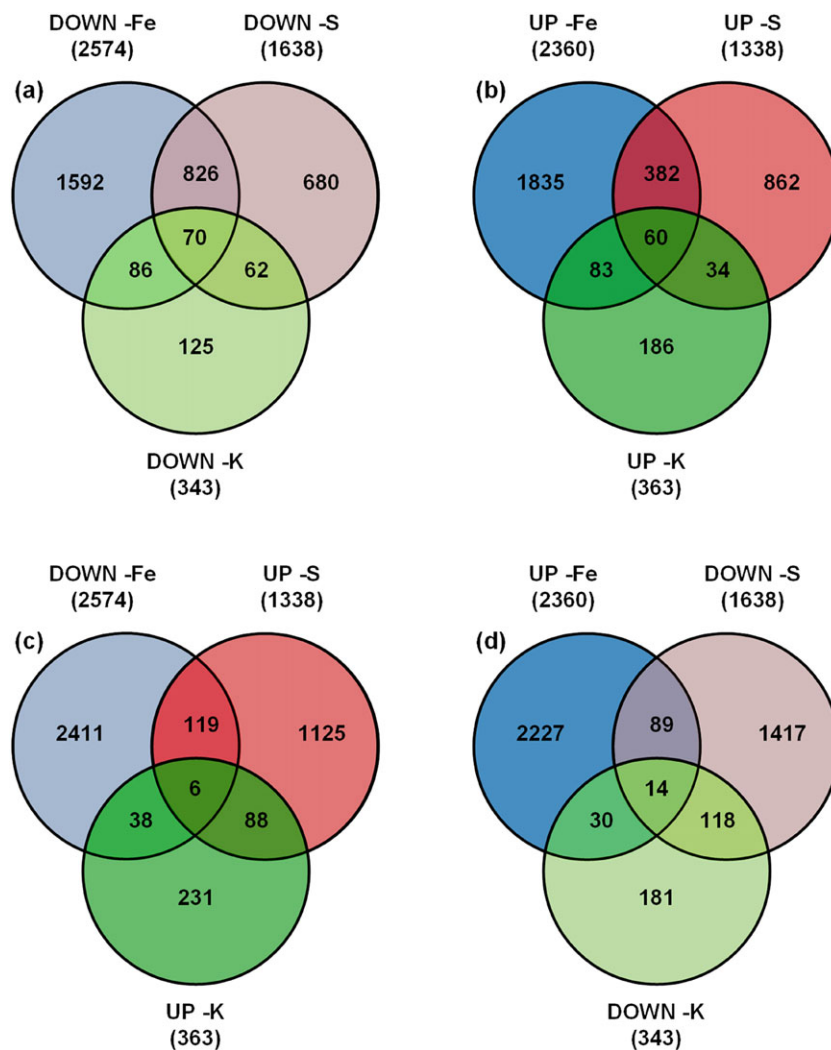


Figure 5. The global transcriptome responds specifically to S, Fe or K deprivation. (a–b) Venn diagrams showing the genes that were down-regulated (a) or up-regulated (b) by iron (-Fe, blue), sulfur (-S, red) and potassium deficiency (-K, green) in roots of 7-week-old Arabidopsis plants. (c–d) Identification of genes that were oppositely regulated by -S and -Fe. Cutoff for definition of a significantly regulated gene when compared with control condition: $P < 0.05$, >1.5 -fold regulated. The total number of up-regulated (UP) or down-regulated (DOWN) is shown in brackets for each treatment.

four biological replicates; Supporting Information Tables S3–S8, which list the 20 most regulated genes of each category. The raw data are uploaded in National Center for Biotechnology Information (NCBI) Gene Expression Omnibus public functional genomics data repository (<http://www.ncbi.nlm.nih.gov/geo/>) under the GEO Accession number (GSE77602)). In general, deficiency of the micronutrient Fe had the highest impact on the total number of genes that were down-regulated (2574; Fig. 5, Supporting Information Table S3a) or up-regulated (2360; Fig. 5, Supporting Information Table S3b) compared with the control condition. S deficiency resulted in down-regulation of 1638 genes (Fig. 5, Supporting Information Table S4a) and up-regulation of 1338 genes in roots (Fig. 5, Supporting Information Table S4b). By contrast, fewer genes were changed by K deficiency (343 down-regulated genes and 363 up-regulated genes, Fig. 5, Supporting Information Table S5a,b). Importantly, approximately 51% of the genes that were down-regulated by -S treatment were also simultaneously

down-regulated by -Fe treatment (826 genes; Fig. 5, Supporting Information Table S6a). The number of -S and -Fe co-induced genes was significantly smaller (382 genes, Fig. 5, Supporting Information Table S6b) and represented 29% of all S-deficiency-induced genes. Less than 4% of S deficiency or Fe deficiency regulated genes were co-regulated within the response to K deficiency. Surprisingly, only 130 genes were regulated in the same manner upon growth limitation by all three nutrients (70 down-regulated and 60 up-regulated; Fig. 5, Supporting Information Table S7a,b). A Gene Set Enrichment Analysis (GSEA) of the respective gene clusters demonstrated that co-regulation of biochemical processes in roots of Arabidopsis by all three nutrients was restricted to the biological processes of disaccharide formation, cell wall organization and response to diverse stimuli (Table 1). However, a note of caution must be added to the interpretation of these GSEA analyses due to the limited number of genes in both clusters.

Table 1. IGene Set Enrichment Analysis (GSEA)

Co-regulated genes under -Fe, -S, and -K				
Biological process	Regulation	Fold enrichment	P-value	FDR (%)
Disaccharide biosynthetic process	↓	26	0.006	7.028
Glycoside biosynthetic process	↓	19	0.001	1.428
Cell wall organization	↓	6.5	0.002	2.676
External encapsulating structure organization	↓	6.1	0.003	3.403
Circadian rhythm	↑	32	0.004	4.530
Red or far red light signalling pathway	↑	19	0.010	11.482
Defence response, incompatible interaction	↑	13	0.021	23.263
Immune response	↑	8.4	0.001	0.695
Response to temperature stimulus	↑	5.8	0.009	10.719
Intracellular signalling cascade	↑	3.7	0.009	11.008
Defence response	↑	3.2	0.009	10.470
Co-regulated genes under -Fe and -S				
Biological process	Regulation	Fold enrichment	P-value	FDR (%)
Response to herbicide	↓	21	5.7E-04	0.892
DNA replication initiation	↓	19	7.2E-07	1.1E-03
Nitrate metabolic process	↓	10	1.3E-03	1.999
Syncytium formation	↓	9.1	8.6E-03	12.693
Starch biosynthetic process	↓	7.5	0.015	21.124
Protein polymerization	↓	7.4	2.9E-04	0.450
Cellulose catabolic process	↓	7.3	1.1E-03	1.759
DNA-dependent DNA replication	↓	6.6	1.5E-05	0.024
Root hair elongation	↓	6.1	8.3E-03	12.186
Plant-type cell wall modification	↓	5.7	0.011	15.605
Microtubule-based process	↓	5.5	1.0E-09	1.6E-06
Glucosinolate biosynthetic process	↓	5.5	0.012	17.484
Response to nematode	↓	4.9	4.8E-04	0.748
Oligopeptide transport	↓	4.5	3.2E-04	0.504
Inorganic anion transport	↓	4.3	5.5E-03	8.324
Cell death	↑	5.1	7.3E-07	1.1E-03
Immune response	↑	4.4	9.7E-08	1.4E-04
Oppositely regulated genes under -Fe and -S				
Biological process	Regulation	Fold enrichment	P-value	FDR (%)
Cellular amino acid catabolic process	↑ Fe ↓ S	27	4.0E-04	0.513
Amine catabolic process	↑ Fe ↓ S	25	4.9E-04	0.623
Glutamine family amino acid metabolic process	↑ Fe ↓ S	15	0.017	19.306
Carboxylic acid catabolic process	↑ Fe ↓ S	14	2.5E-03	3.211
Ion homeostasis	↑ Fe ↓ S	13	3.6E-03	4.540
Transition metal ion transport	↑ Fe ↓ S	12	0.024	26.743
Cellular response to sulfur starvation	↓ Fe ↑ S	125	0.016	18.043
Regulation of glucosinolate biosynthetic process	↓ Fe ↑ S	100	0.019	22.021
Sulfate assimilation/cysteine biosynthetic process	↓ Fe ↑ S	54	1.3E-03	1.678
Serine family amino acid biosynthetic process	↓ Fe ↑ S	25	6.1E-03	7.492
Transmembrane receptor protein Tyr kinase signalling	↓ Fe ↑ S	7.7	0.014	16.800

Enriched GO biological processes, *P*-value and false discovery rates (FDR in percent) are reported.

The GSEA of co-regulated genes under -Fe and -S conditions revealed significant down-regulation of 15 biological processes (Table 1) of which responses to herbicide and DNA replication initiation were most enriched (fold enrichment > 15-fold). Most of these processes were down-regulated and only two, cell death and immune response, were up-regulated by S and Fe deficiency (Table 1).

The gene clusters in the Venn diagram (Fig. 5c,d) that were oppositely regulated by both nutrients were analysed (Fig. 5c, d and Supporting Information Table S8a,b): the GSEA analysis of the two gene clusters (Table 1) revealed 13 biological processes, including the ‘cellular response to S-starvation’, the ‘regulation of glucosinolate biosynthetic process’ and the

‘transition metal ion transport’. The data demonstrated that the cross-talk between Fe and S pathway regulation in roots consisted of a ‘co-regulation component’ (i.e. expression change in the same direction by -Fe and -S) and an ‘opposing regulation component’ (i.e. expression up at -Fe and down at -S, or vice versa). The ‘opposing regulation component’ was in terms of number of regulated genes smaller than the co-regulation component but included the assimilation pathways for Fe and S (Fig. 6). In particular, opposing regulation upon Fe and S deficiency was observed for important key components of the sulfate -efficiency response (*SULTRI;1*, all *APR* genes) and the Fe import machinery (*FRO2* and *IRT1*) and NA synthesis (*NAS4*). Regulation of the Fe assimilation

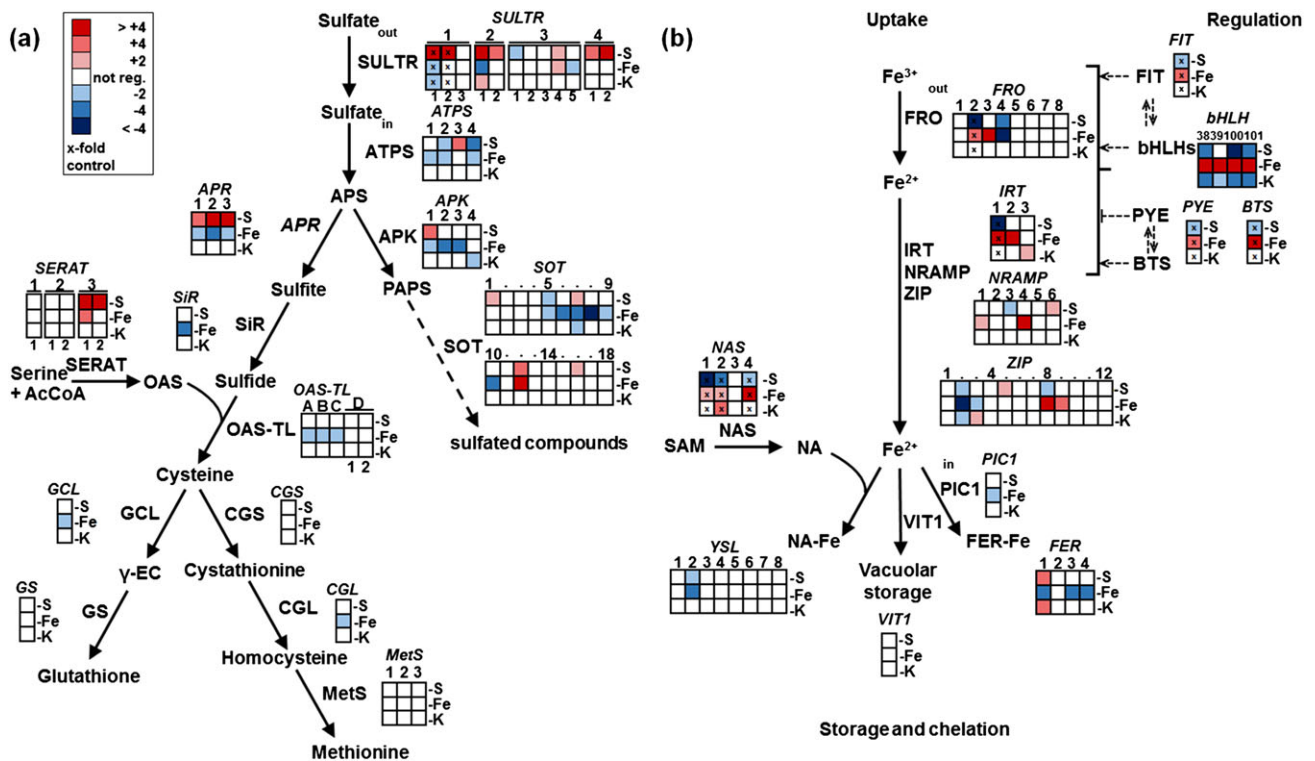


Figure 6. Genes of the sulfur and iron assimilation pathways are oppositely regulated by iron and sulfur deprivation but almost unaffected by K limitation. (a–b) Graphical presentation of the sulfate (a) and the iron assimilation pathway (b). Transcript levels of genes (italics) that catalyse single-step reactions (continuous arrows) or act as positive (dashed arrows) or negative regulators (dashed lines) are indicated by colour code. White represents no significant change in comparison to control condition ($P < 0.05$; >1.5 -fold regulated, $n = 4$). Metabolites are shown in bold. Abbreviations of metabolites and gene names are provided in text. Double arrows depict interaction between encoded proteins. The transcriptional regulation of gene-family members and important low abundant transcription factors has been additionally quantified by qRT-PCR in order to exclude cross-hybridization artifacts by application of the micro-array technology (cross).

machinery in response to S deficiency may be explained by the down-regulation of the key transcription factor network of Fe-deficiency response upon S deficiency (e.g. *BTS* and the *bHLH* transcription factors 38, 39, 100, 101, *FIT* and *PYE*; Brumbarova *et al.* 2015). In contrast to *FIT*, *PYE* and *BTS*, which were only regulated by S and Fe, the *bHLH* transcription factors 38, 39, 100 and 101 were also affected by K deficiency. Surprisingly, Fe deficiency resulted in the down-regulation of 14 genes encoding for proteins involved in sulfate assimilation that were not regulated in response to S deficiency, including *SiR*, *APK1*, *OAS-TL A* and *OAS-TL B* (Fig. 6a, Supporting Information Table S9). Similarly, three genes of the Fe assimilation pathway were only regulated by S deficiency and not by Fe deficiency (*NRAMP3* was down-regulated, while *NRAMP6* and *ZIP5* were up-regulated; Fig. 6b, Supporting Information Table S10). Several of the 14 identified genes were also significantly down-regulated to various degrees in publicly available data sets (Genevestigator® V3; Hruz *et al.* 2008; <https://genevestigator.com/gv/plant.jsp>) after application of Fe deficiency (e.g. *SiR* and *OAS-TL A*; Supporting Information Table S8). There is a trend for down-regulation of this set of sulfate assimilation genes by Fe deficiency, but such a trend lacks statistical significance. Other studies also confirm that the expression of these genes is not affected by sulfur

deficiency (Supporting Information Table S9). In the present study, the identified impact of long-term S deficiency on the regulation of Fe assimilation genes was not statistically significant for the available data sets for short-term S deficiency (Supporting Information Table S9), indicating a specific effect of the long-term S deficiency.

The GSEA of genes that were specifically regulated by only one nutrient deprivation and not the other applied deprivation conditions uncovered several nutrient-specific regulated biological processes in roots of Arabidopsis (Supporting Information Tables S11–S13). Most interestingly, pathways for methylation of DNA and chromosome condensation were down-regulated upon S deficiency and ABA responsive genes were only up-regulated in K-deficiency, which is in agreement with the strong accumulation of ABA in K-deprived roots.

To provide unbiased statistical support for the significant cross-talk between the Fe-deficiency and S-deficiency response, a hierarchical clustering of the transcriptome (Supporting Information Fig. S3a) and the metabolome data matrix was performed (Supporting Information Fig. S3b) by using the Pearson correlation coefficient computed for every possible sample matrix comparison. Importantly, -Fe and -S treated samples cluster together in the dendrogram and were separated from control and K-deficient samples.

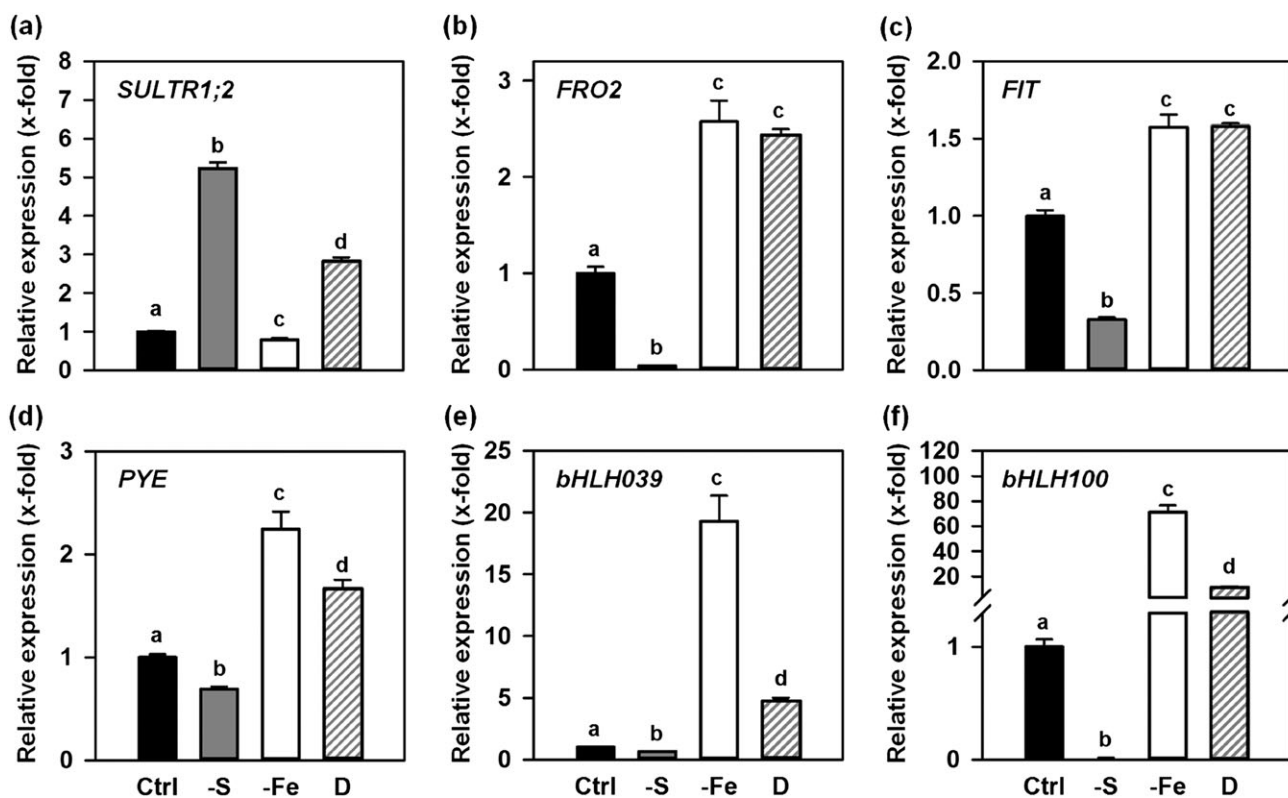


Figure 7. Impact of single S or Fe and combined S and Fe deficiency on the transcription of sulfur and iron uptake-related genes. (a–f) Transcript levels of the high affinity sulfate transporter *SULTR1;2* (a), the ferric-chelate reductase oxidase *FRO2* (b) and the Fe metabolism regulating transcription factors *FIT* (c), *PYE* (d), *bHLH039* (e) and *bHLH100* (f) in roots of 7-week old Arabidopsis wild-type plants hydroponically grown on full medium (Ctrl, black) or medium depleted for S (-S, dark grey), Fe (-Fe, white) or both nutrients (D, dashed grey, white) as specified in material and methods. Data are means \pm SE of four individual replicates. Lettering indicates statistical differences by ANOVA ($P < 0.05$) as determined by Student–Newman–Keuls test.

Impact of simultaneous Fe and S deficiency on the expression of iron and sulfur uptake and homeostasis genes

A double-deficiency approach was applied to assess the impact of S supply on the Fe-deficiency response and vice versa. This independent experiment confirmed the opposing regulation of the S and Fe uptake transporter machinery upon single deficiency of either Fe or S as described earlier and by Forieri *et al.* (2013). The combined starvation of S and Fe overcame the negative impact of Fe deficiency on transcription of the S-uptake system (*SULTR1;2*; Fig. 7a) as well as the negative impact of single S deficiency on the Fe assimilation pathway (*FRO2*, *NASI* and *NAS4*; Fig. 7b and Supporting Information Fig. S4) and resulted in significant induction of both uptake systems. The down-regulation of Fe-metabolism regulating transcription factors upon -S was also absent when -S and -Fe were simultaneously applied (Fig. 7c–f). Induction of *FIT* by combined S and Fe deficiency was indistinguishable from induction by -Fe (Fig. 7c), while the Fe deficiency-induced up-regulation of *PYE*, *bHLH039* and *bHLH100* was dampened by -S during combined application of -S and -Fe (Fig. 7d–f). This suggests that the specific need for one of the nutrients overrules the co-down-regulation by the partner nutrient.

DISCUSSION

In this study, long-term S-deficiency, Fe-deficiency and K-deficiency treatments have been applied to the model plant *Arabidopsis thaliana* to dissect general nutrient-depletion-induced responses from specific cross-talk between S and Fe metabolism. In accordance with a systematic study on the differences in reorganization of root architecture under different nutrient deficiencies (Gruber *et al.* 2013), a specific increase of the root to shoot ratio by S deficiency but not by deficiency of the other nutrients, Fe or K, was found. In combination with the nutrient deficiency-specific leaf phenotypes (Fig. 1), these results indicated the presence of rather specific adaptations in both organs rather than a global nutrient depletion-induced response. Surprisingly, only 130 genes were regulated in common by all three nutrient-deficiency stresses in roots. The down-regulated genes of this category were enriched in pathways for production of disaccharides and the organization of the cell wall, while the up-regulated genes were distributed in response pathways to diverse abiotic and biotic stimuli. Indeed, global transcriptomics and comprehensive metabolite analyses revealed specific transcriptional and metabolic adaptations in response to the three nutrient deficiencies. These responses included up-regulation of genes encoding the respective

nutrient uptake machinery, for example *SULTRI;1* in response to S deficiency and *IRT1* in response to Fe deficiency (Eide *et al.* 1996, Hirai *et al.* 2003). Surprisingly, the high affinity S-transporter, *SULTRI;1*, was significantly down-regulated by Fe deficiency. Similarly, S depletion caused repression of Fe uptake by *IRT1*. Such an opposing regulation of the high affinity *SULTR* system by Fe and S supply was also indicated by studies of 2-week-old barley roots (Astolfi *et al.* 2012). The down-regulation of the sulfate uptake capacity by Fe-deficiency can be interpreted as an adaptation to the lowered need of the partner nutrient S for synthesis of Fe-S clusters (Vigani & Briat 2015), when Fe is limiting. The same is true for the down-regulation of the gene of *IRT1* in response to S deficiency. That such a co-depression of uptake machinery for the partner nutrient occurred in Arabidopsis was also strongly indicated from the unchanged total Fe content of S-deprived plants when compared with control plants, which produced significantly more root and shoot biomass than the S-deprived plants. However, the transcriptional down-regulation of high affinity sulfate transporters (*SULTRI* group) by Fe deficiency did not occur in tomato roots, although Fe-deprived tomato plants grew slower and had lowered total S contents than control plants (Zuchi *et al.* 2015). Apparently, in tomato, another mechanism must be responsible for the significant down-regulation of sulfate uptake during Fe deficiency. In our study with Arabidopsis, transcriptional co-depression of the sulfate assimilation pathway by Fe deficiency is at least partially achieved by specific signal transduction systems, since it affected 14 genes that were not regulated by S deficiency at the transcriptional level. In the case of co-depression of the Fe assimilation pathway by S deficiency, down-regulation of *IRT1* correlated with down-regulation of the known Fe transcription factor network of *FIT*, *PYE*, *BTS*, *bHLH38*, *bHLH100* and *bHLH101*, that also controls *IRT1* transcription upon Fe deficiency (Colangelo & Guerinot 2004). How S-deficiency results in down-regulation of this transcription factor network and in particular *FIT* is as yet unknown. Combined depletion of S and Fe resulted in the typical induction of both nutrient uptake systems. Thus, one canonical nutrient-deficiency response signal transduction cascade (e.g. induction of *FIT* in combined S and Fe deficiency; Colangelo & Guerinot 2004) can overrule the co-depression between both pathways.

Knowledge about the general control of the root nutrient-assimilation machineries by phytohormones is scarce (Iqbal *et al.* 2013). The determination of stress-related phytohormones revealed a nutrient-deficiency specific signature that was conserved in roots and leaves and is likely to contribute to regulation of the transcriptional response: out of the analysed phytohormones, only SA was found to be oppositely regulated in response to Fe and S depletion. Up-regulation of SA might indeed contribute to up-regulation of the sulfur-uptake machinery in S-deprived roots of Arabidopsis, since it promotes the activity of SAT and accumulation of its product OAS (Freeman *et al.* 2005), the known inducer for transcription of *SULTRI;1* and a distinct set of S-metabolism-related genes (Hubbarten *et al.* 2012). Indeed, OAS accumulated dramatically in roots of S-depleted plants and is an accepted marker of S deficiency (reviewed in Takahashi *et al.* 2011).

However, OAS cannot be the sole signal for regulation of *SULTRI;1* transcription, as demonstrated by careful analysis of *SULTR* transcription patterns in response to various stimuli by different groups (Rouached *et al.* 2008) and the minor increase of OAS in response to Fe deficiency observed in this study. The strong induction of the established Fe-deficiency marker genes *IRT1* and *FRO2* upon Fe-deficiency can be explained by induction of the transcription factor *FIT* (Colangelo & Guerinot 2004) and the release from transcriptional suppression by JA (Maurer *et al.* 2011), which decreased significantly more in roots of Fe-depleted plant than in plants depleted of S or K. Since *FIT* stability is regulated by ethylene signalling via *EIN3/EIL1* axis (Lingam *et al.* 2011) and nitric oxide (Meiser *et al.* 2011), a complex network of stimulating and repressing signal molecules exists in roots to regulate *FIT* abundance in response to stresses.

The specific accumulation of ABA in K-deprived Arabidopsis roots (Fig. 4) provides a molecular explanation for the strong and exclusive induction of ABA-responsive genes upon K-deficiency (Supporting Information Table S12). Such an up-regulation of ABA has also been found in K-deficient maize roots (Schraut *et al.* 2005). The latter indicates an important signalling function of ABA in roots of monocotyledonous and dicotyledonous plants during K-deficiency-induced stress. Part of this signalling function is the adaptation of root function by nutrient-deficiency-induced endodermal differentiation (Barberon *et al.* 2016). It may be concluded from these findings that the signature of the three stress-related hormones ABA, JA and SA contribute to the transcriptional regulation of nutrient-deficiency responses in plant roots.

However, it is likely that other mechanisms and/or primary metabolites also contribute to regulation of the observed transcriptional response. Very recently, epigenetic regulation by DNA methylation has been shown to regulate a significant part of the phosphate-deficiency response (Yong-Villalobos *et al.* 2015). Similarly, down-regulation of the DNA methylation pathway as a novel and specific response to prolonged S-deficiency was identified in the present study (Table 1). Decreased availability of the methyl group donor SAM and its precursor Met has been previously demonstrated during S deficiency and was supposed to limit the DNA methylation capacity (Nikiforova *et al.* 2005). However, careful analysis of the methylation index (SAM/SAH ratio; Fig. 3) puts a note of caution to this interpretation.

Remarkably, Fe deficiency has transcriptional control over a specific set of S-assimilation genes, which in terms of number of regulated genes (27 for Fe), is comparable to regulation of the core S metabolism by S deficiency (22 genes; Fig. 6). Fe deficiency does not only down-regulate canonical S-deficiency response genes (*SULTRI;1* and *APR* genes) but also many S-metabolism-related genes downstream of *APR* including *SiR* (Fig. 6). *SiR* activity has been identified as a bottleneck in the S-assimilation pathway, although the transcript level or protein abundance are not altered by sulfate deficiency (Khan *et al.* 2010). Transgenic down-regulation of *SiR* transcript levels in the *sir1-1* mutant to similar levels determined in wild-type roots after Fe deficiency resulted in a >15-fold decrease of S incorporation into cysteine and a significant retardation of

growth (Khan *et al.* 2010). Thus, Fe-deficiency-induced down-regulation of SiR might be one determinant for decreased S flux into cysteine, the sole S donor for Fe-S cluster biosynthesis (Balk & Schaedler 2014), and will contribute to co-depression of the sulfur assimilation pathway.

CONCLUSION

Comprehensive metabolite analyses uncovered a nutrient-deficiency-specific signature of the stress-related hormones ABA, JA and SA. These established signal molecules are likely to contribute, together with altered levels of known key primary metabolites, to the regulation of the specific transcriptional response of the root to growth limitation by starvation of distinct nutrients. The application of global transcriptomics allowed the dissection of S-specific-deficiency, Fe-specific-deficiency and K-specific-deficiency responses from a hypothesized global nutrient-depletion response that was, if present at all, almost entirely restricted to disaccharide formation and cell wall organization in roots of *Arabidopsis*. Furthermore, this study demonstrates a consistent connection between S and Fe metabolism at both transcriptomic and metabolic level. The response to K deficiency was shown not to be part of this cross-talk, providing evidence for the specificity of the Fe and S network. The fact that Fe deficiency controls a distinct subset of sulfur-assimilation genes that are not regulated by S deficiency demonstrates that at least two independent signal transduction cascades control this network. This study sets the stage for the analysis of stress-hormone signalling within the nutrient-deficiency response of plants roots by application of reverse genetic tools available in *Arabidopsis*.

MATERIAL AND METHODS

Growth conditions and phenotype determination

Arabidopsis thaliana (Columbia-0 accession) seeds were surface-sterilized with 70% (v/v) ethanol, washed with sterile ddH₂O and subsequently placed in individual micro-centrifuge tubes containing half-strength Hoagland solution [2.5 mM Ca(NO₃)₂, 2.5 mM KNO₃, 0.5 mM MgSO₄, 0.5 mM KH₂PO₄ and 10 μM Fe³⁺ complexed with *N,N'*-di-(2-hydroxybenzoyl)-ethylenediamine-*N,N'*-diacetate (FeHBED) and 25 μM H₃BO₃, 2.25 M MnCl₂, 1.9 μM ZnSO₄, 0.15 μM CuCl₂ and 0.05 μM (NH₄)₆Mo₇O₂₄, pH 5.8 to 6.0] supplemented with 0.6% (w/v) agar inserted in small boxes (0.4 L) according to Tocquin *et al.* (2003). For the K starvation treatment, K concentration in the Hoagland media was reduced 10 times and replaced with Na₂HPO₄ and Ca(NO₃)₂ to avoid phosphate or nitrate starvation. After 2 d of stratification at 4 °C boxes were placed in the growth cabinet with an 8 h/16 h d/night cycle at light intensity of 120 μmol m⁻² s⁻¹ and 22 °C and 18 °C, respectively, and maintained there for 2 weeks. Individual plants were then transferred into 6 L boxes containing half-strength Hoagland solution and subjected for 5 weeks to nutrient deficiency. For the sulfur-deficiency treatment (-S), MgSO₄ concentration was lowered

to 1 μM. The absent 499 μM MgSO₄ was replaced with MgCl₂. For the Fe deficiency (-Fe) treatment, FeHBED concentration was decreased to 0.1 μM. These two treatments were combined to obtain the double nutrient deficiency (D). For the potassium-deficiency treatment (-K), K⁺ was omitted completely from the media and replaced with Na₂HPO₄ and Ca(NO₃)₂. Media were exchanged weekly and additionally 24 h before harvesting of plants.

Determination of metabolites, nutrients and phytohormones

Anions, OAS, thiols, NA and adenosines were extracted from around 50 mg of frozen root tissue and quantified according to Heeg *et al.* (2008), Klatt *et al.* (2009) and Burstenbinder *et al.* (2007).

Nutrient concentrations were determined by inductively coupled plasma-optical emission spectrometry (ICP-OES) (Applied Research Laboratories, Vallaire, Ecublens, Switzerland) as described in Shahbaz *et al.* (2011).

Amino acids were extracted from 100 mg of frozen root material with 1 mL of 80% methanol solution, and the resulting extract was diluted in a ratio of 1:10 (v/v) in water containing the ¹³C, ¹⁵N labelled amino acid mix (Isotec, Miamisburg, USA). Amino acids in the diluted extracts were directly analysed by LC-MS/MS as described in Docimo *et al.* (2012). Phytohormones were quantified from the undiluted methanol extract according to Vadassery *et al.* (2012). In both cases, an API5000 mass spectrometer (Applied Biosystems) was used for quantification. Glucosinolates were determined from the methanol extract after addition of 0.05 mM 4-hydroxybenzylglucosinolate as internal standard by HPLC-UV as described in Burow *et al.* (2006).

RNA extraction and analysis of transcript levels

Total RNA was extracted from 50 mg of frozen root material using the peqGOLD Total RNA Kit (peqGOLD, Erlangen, Germany) according to the manufacturer's instruction.

Global transcriptome analysis was performed with the *Arabidopsis thaliana* gene chip (AraGene-1_0-st-type) from Affymetrix (High Wycombe, UK) according to (Linster *et al.* 2015) with the only exception that the newest TAIR-based custom CDF-Version 18 instead of version 16 was used for annotation of genes. GSEA was used to determine whether defined sets of genes exhibit a statistically significant bias in their distribution within a ranked gene list using the software *DAVID Bioinformatics Resources 6.7* (<http://david.abcc.ncifcrf.gov>). Pathways belonging to various cell functions such as cell cycle or apoptosis were obtained from public external databases (KEGG, <http://www.genome.jp/kegg>).

Quantitative real time-PCR (qRT-PCR) analysis was performed by using the qPCRBIOSyGreen Mix Lo-ROX (PCR Biosystems, London, UK) in the Rotor-Gene Q cyclor (Qiagen, Hilden, Germany). The data were evaluated by using the Rotor-Gene Q Software 2.0.2 (Qiagen) after the generation of standard curves. The gene *TIP41-like*

(*At4g34270*) was used as a reference gene based on previous unbiased screens for genes whose transcription are not affected by diverse stress conditions (Czechowski *et al.* 2005), including nutrient deprivation (Fe deficiency; Han *et al.* 2013). Gene specific primers used for qRT-PCR are listed in Supporting Information Table S13.

Statistical analysis

Statistical analysis was performed by using the software SigmaPlot 12.0. Different data sets were analysed for statistical significance with the analysis of variance (ANOVA) followed by the Student–Newman–Keuls or Keul's *post hoc* test. Different letters in the figures indicate significant difference ($P < 0.05$).

Accession numbers

The microarray data sets are uploaded to the NCBI GEO database under the GEO Accession number (GSE77602).

ACKNOWLEDGMENTS

We thank the Metabolomics Core Technology Platform Heidelberg funded by the DFG Excellence initiative for excellent support during metabolite analysis.

AUTHOR CONTRIBUTIONS

I.F. performed most of the experiments and contributed to writing of the manuscript with M.M. M.R. and M.J.H. determined phytohormones and nutrient contents, respectively. C. S. and N.G. acquired transcriptome data and performed statistical analysis. M.W. and R.H. supervised I.F. and wrote the manuscript.

REFERENCES

Amtmann A. & Armengaud P. (2009) Effects of N, P, K and S on metabolism: new knowledge gained from multi-level analysis. *Curr Opin Plant Biol* **12**, 275–283.

Astolfi S., Zuchi S., Hubberten H.-M., Pinton R. & Hoefgen R. (2010) Supply of sulphur to S-deficient young barley seedlings restores their capability to cope with iron shortage. *J. Exp. Bot.* **61**, 799–806.

Astolfi S., Zuchi S., Neumann G., Cesco S., di Toppi L.S. & Pinton R. (2012) Response of barley plants to Fe deficiency and Cd contamination as affected by S starvation. *Journal of Experimental Botany* **63**, 1241–1250.

Balk J. & Schaedler T.A. (2014) Iron cofactor assembly in plants. *Annu Rev Plant Biol* **65**, 125–153.

Barberon M., Vermeer J.E., De Bellis D., Wang P., Naseer S., Andersen T.G., ... Geldner N. (2016) Adaptation of root function by nutrient-induced plasticity of endodermal differentiation. *Cell*.

Bittner F. (2014) Molybdenum metabolism in plants and crosstalk to iron. *Front Plant Sci* **5**, 1–6.

Brumbarova T., Bauer P. & Ivanov R. (2015) Molecular mechanisms governing Arabidopsis iron uptake. *Trends Plant Sci* **20**, 124–133.

Burrow M., Muller R., Gershenzon J. & Wittstock U. (2006) Altered glucosinolate hydrolysis in genetically engineered *Arabidopsis thaliana* and its influence on the larval development of *Spodoptera littoralis*. *J Chem Ecol* **32**, 2333–2349.

Burstenbinder K., Rzewuski G., Wirtz M., Hell R. & Sauter M. (2007) The role of methionine recycling for ethylene synthesis in Arabidopsis. *Plant J* **49**, 238–249.

Chan K.X., Wirtz M., Phua S.Y., Estavillo G.M. & Pogson B.J. (2013) Balancing metabolites in drought: the sulfur assimilation conundrum. *Trends Plant Sci* **18**, 18–29.

Colangelo E.P. & Gueriot M.L. (2004) The essential basic helix-loop-helix protein FIT1 is required for the iron deficiency response. *Plant Cell* **16**, 3400–3412.

Czechowski T., Stitt M., Altmann T., Udvardi M.K. & Scheible W.R. (2005) Genome-wide identification and testing of superior reference genes for transcript normalization in Arabidopsis. *Plant Physiol* **139**, 5–17.

Docimo T., Reichelt M., Schneider B., Kai M., Kunert G., Gershenzon J. & D'Auria J.C. (2012) The first step in the biosynthesis of cocaine in *Erythroxylum coca*: the characterization of arginine and ornithine decarboxylases. *Plant Mol Biol* **78**, 599–615.

Eide D., Broderius M., Fett J. & Gueriot M.L. (1996) A novel iron-regulated metal transporter from plants identified by functional expression in yeast. *Proc Natl Acad Sci U S A* **93**, 5624–5628.

Forieri I., Wirtz M. & Hell R. (2013) Toward new perspectives on the interaction of iron and sulfur metabolism in plants. *Front Plant Sci* **4**, 1–5.

Freeman J.L., Garcia D., Kim D., Hopf A. & Salt D.E. (2005) Constitutively elevated salicylic acid signals glutathione-mediated nickel tolerance in *Thlaspi* nickel hyperaccumulators. *Plant Physiol* **137**, 1082–1091.

Garcia M.J., Romera F.J., Lucena C., Alcantara E. & Perez-Vicente R. (2015) Ethylene and the regulation of physiological and morphological responses to nutrient deficiencies. *Plant Physiol* **169**, 51–60.

Gruber B.D., Giehl R.F.H., Friedel S. & von Wirén N. (2013) Plasticity of the Arabidopsis root system under nutrient deficiencies. *Plant Physiology* **163**, 161–179.

Han B., Yang Z., Samma M.K., Wang R. & Shen W. (2013) Systematic validation of candidate reference genes for qRT-PCR normalization under iron deficiency in Arabidopsis. *Biometals* **26**, 403–413.

Heeg C., Kruse C., Jost R., Gutensohn M., Ruppert T., Wirtz M. & Hell R. (2008) Analysis of the Arabidopsis *O*-acetylserine(thiol)lyase gene family demonstrates compartment-specific differences in the regulation of cysteine synthesis. *Plant Cell* **20**, 168–185.

Hirai M., Fujiwara T., Awazuhara M., Kimura T., Noji M. & Saito K. (2003) Global expression profiling of sulfur-starved Arabidopsis by DNA microarray reveals the role of *O*-acetyl-L-serine as a general regulator of gene expression in response to sulfur nutrition. *Plant J.* **33**, 651–663.

Hirai M.Y., Yano M., Goodenowe D.B., Kanaya S., Kimura T., Awazuhara M., ... Saito K. (2004) Integration of transcriptomics and metabolomics for understanding of global responses to nutritional stresses in *Arabidopsis thaliana*. *Proc. Natl. Acad. Sci. U. S. A.* **101**, 10,205–10,210.

Hruz T., Laule O., Szabo G., Wessendorp F., Bleuler S., Oertle L., ... Zimmermann P. (2008) Genevestigator V3: a reference expression database for the meta-analysis of transcriptomes. *Advances in Bioinformatics* doi:10.1155/2008/420747.

Hubberten H., Klie S., Caldana C., Degenkolbe T., Willmitzer L. & Hoefgen R. (2012) Additional role of *O*-acetylserine as a sulfur status-independent regulator during plant growth. *Plant J* **70**, 666–677.

Iqbal N., Trivellini A., Masood A., Ferrante A. & Khan N.A. (2013) Current understanding on ethylene signaling in plants: the influence of nutrient availability. *Plant Physiol Biochem* **73**, 128–138.

Khan M.S., Haas F.H., Allboje S.A., Moghaddas G.A., Bauer A., Fellenberg K., ... Hell R. (2010) Sulfite reductase defines a newly discovered bottleneck for assimilatory sulfate reduction and is essential for growth and development in *Arabidopsis thaliana*. *Plant Cell* **22**, 1216–1231.

Klatte M., Schuler M., Wirtz M., Fink-Straube C., Hell R. & Bauer P. (2009) The analysis of Arabidopsis nicotianamine synthase mutants reveals functions for nicotianamine in seed iron loading and iron deficiency responses. *Plant Physiol* **150**, 257–271.

Koprivova A. & Kopriva S. (2016) Hormonal control of sulfate uptake and assimilation. *Plant Mol Biol* **91**, 617–627.

Liang C., Tian J. & Liao H. (2013) Proteomics dissection of plant responses to mineral nutrient deficiency. *PROTEOMICS* **13**, 624–636.

Lingam S., Mohrbacher J., Brumbarova T., Potuschak T., Fink-Straube C., Blondel E., Genschik P. & Bauer P. (2011) Interaction between the bHLH transcription factor FIT and ETHYLENE INSENSITIVE3/ETHYLENE INSENSITIVE3-LIKE1 reveals molecular linkage between the regulation of iron acquisition and ethylene signaling in Arabidopsis. *Plant Cell* **23**, 1815–1829.

Linster E., Stephan I., Bienvenu W.V., Maple-Grodum J., Myklebust L.M., Huber M., ... Wirtz M. (2015) Downregulation of *N*-terminal acetylation triggers ABA-mediated drought responses in Arabidopsis. *Nat Commun* doi:10.1038/ncomms8640.

Maruyama-Nakashita A., Nakamura Y., Yamaya T. & Takahashi H. (2004) A novel regulatory pathway of sulfate uptake in Arabidopsis roots: implication

of CRE1/WOL/AHK4-mediated cytokinin-dependent regulation. *Plant J* **38**, 779–789.

Maurer F., Muller S. & Bauer P. (2011) Suppression of Fe deficiency gene expression by jasmonate. *Plant Physiol Biochem* **49**, 530–536.

Meiser J., Lingam S. & Bauer P. (2011) Posttranslational regulation of the iron deficiency basic helix-loop-helix transcription factor FIT is affected by iron and nitric oxide. *Plant Physiol* **157**, 2154–2166.

Nikiforova V.J., Kopka J., Tolstikov V., Fiehn O., Hopkins L., Hawkesford M.J., Hesse H. & Hoefgen R. (2005) Systems rebalancing of metabolism in response to sulfur deprivation, as revealed by metabolome analysis of Arabidopsis plants. *Plant Physiol* **138**, 304–318.

Rouached H., Wirtz M., Alary R., Hell R., Arpat A.B., Davidian J.-C.E., Fourcroy P. & Berthomieu P. (2008) Differential regulation of the expression of two high-affinity sulfate transporters, SULTR1.1 and SULTR1.2 in Arabidopsis. *Plant Physiology* **147**, 897–911.

Sauter M., Moffatt B., Saechao M.C., Hell R. & Wirtz M. (2013) Methionine salvage and S-adenosylmethionine: essential links between sulfur, ethylene and polyamine biosynthesis. *Biochem J* **451**, 145–154.

Schachtman D.P. & Shin R. (2007) Nutrient sensing and signaling: NPKS. *Annu Rev Plant Biol* **58**, 47–69.

Schraut D., Heilmeyer H. & Hartung W. (2005) Radial transport of water and abscisic acid (ABA) in roots of Zea mays under conditions of nutrient deficiency. *J Exp Bot* **56**, 879–886.

Shahbaz M., Hwei T.M., Stuver C.E.E., Koralewska A., Posthumus F.S., Venema J.H., ... De Kok L.J. (2011) Copper exposure interferes with the regulation of the uptake, distribution and metabolism of sulfate in Chinese cabbage. *Journal of Plant Physiology* **167**, 438–446.

Takahashi H., Kopriva S., Giordano M., Saito K. & Hell R. (2011) Sulfur assimilation in photosynthetic organisms: molecular functions and regulations of transporters and assimilatory enzymes. *Annu Rev Plant Biol* **62**, 157–184.

Tocquin P., Corbesier L., Havelange A., Pieltain A., Kurtem E., Bernier G. & Perilleux C. (2003) A novel high efficiency, low maintenance, hydroponic system for synchronous growth and flowering of *Arabidopsis thaliana*. *BMC Plant Biol* doi:10.1186/1471-2229-3-2.

Vadassery J., Reichelt M., Hause B., Gershenzon J., Boland W. & Mithöfer A. (2012) CML42-mediated calcium signaling coordinates responses to Spodoptera herbivory and abiotic stresses in Arabidopsis. *Plant Physiology* **159**, 1159–1175.

Vigani G. & Briat J.F. (2015) Impairment of respiratory chain under nutrient deficiency in plants: does it play a role in the regulation of iron and sulfur responsive genes? *Front Plant Sci* **6**, doi:10.3389/fpls.2015.01185.

Wang Y. & Wu W.H. (2013) Potassium transport and signaling in higher plants. *Annu Rev Plant Biol* **64**, 451–476.

Wang Y.H., Garvin D.F. & Kochian L.V. (2002) Rapid induction of regulatory and transporter genes in response to phosphorus, potassium, and iron deficiencies in tomato roots. Evidence for cross talk and root/rhizosphere-mediated signals. *Plant Physiol* **130**, 1361–1370.

Watanabe M., Hubberten H.-M., Saito K. & Hoefgen R. (2010) General regulatory patterns of plant mineral nutrient depletion as revealed by serat quadruple mutants disturbed in cysteine synthesis. *Mol Plant* **3**, 438–466.

Yong-Villalobos L., González-Morales S.I., Wrobel K., Gutiérrez-Alanis D., Cervantes-Peréz S.A., Hayano-Kanashiro C., ... Herrera-Estrella L. (2015) Methylole analysis reveals an important role for epigenetic changes in the regulation of the Arabidopsis response to phosphate starvation. *Proceedings of the National Academy of Sciences* **112**, E7293–E7302.

Zuchi S., Watanabe M., Hubberten H.M., Bromke M., Osorio S., Fernie A.R., ... Astolfi S. (2015) The interplay between sulfur and iron nutrition in tomato. *Plant Physiol* **169**, 2624–2639.

Received 19 May 2016; received in revised form 6 September 2016; accepted for publication 19 September 2016

SUPPORTING INFORMATION

Additional Supporting Information may be found in the online version of this article at the publisher's web-site:

Figure S1. Effect of different nutrient deficiencies on amino acid profiling.

Figure S2. Effect of different nutrient deficiencies on jasmonic acid precursor and its derivatives.

Figure S3. The S and Fe deficiency-induced metabolome and transcriptome share higher correlation than the control and the K deficiency-induced metabolome and transcriptome.

Figure S4. Effect of single and double nutrient deficiencies on the expression of *NAS* isoforms.

Table S1. Profile of individual glucosinolates in roots of nutrient deficient Arabidopsis plants.

Table S3. List of the 20 most (a) down-regulated and (b) up-regulated genes under Fe limitation in roots of Arabidopsis plants.

Table S4. List of the 20 most (a) down-regulated and (b) up-regulated genes under S limitation in roots of Arabidopsis plants.

Table S5. List of the 20 most (a) down-regulated and (b) up-regulated genes under K limitation in roots of Arabidopsis plants.

Table S6. List of the 20 most (a) down-regulated and (b) up-regulated genes under Fe and S limitation in roots of Arabidopsis plants.

Table S7. List of the 20 most (a) down-regulated and (b) up-regulated genes under Fe, S and K limitation in roots of Arabidopsis plants.

Table S8. List of the 20 (a) most up-regulated genes under -S and down-regulated genes under -Fe and (b) most down-regulated genes under -S and up-regulated genes under -Fe in roots of Arabidopsis plants.

Table S9. Analysis in public available databases (Genevestigator® V3) of the expression in roots of the 14 genes belonging to S assimilation that were specifically down-regulated by -Fe.

Table S10. Analysis in public available databases (Genevestigator® V3) of the expression in roots of the three genes belonging to Fe assimilation that were specifically regulated by -S.

Table S11. Gene Set Enrichment Analysis (GSEA) of down-regulated or up-regulated genes specifically under Fe limitation.

Table S12. GSEA of down-regulated or up-regulated genes specifically under S limitation.

Table S13. GSEA of down-regulated or up-regulated genes specifically under K limitation.

Table S14. List of primers used for quantitative real time-PCR. Supporting Information Table S2. Mean values were calculated from the normalized expression values of the four biological replicates in the microarray analysis of Arabidopsis roots and expressed as log₂.